NANO LETTERS

Letter

pubs.acs.org/NanoLett

Hybrid Multiferroic Nanostructure with Magnetic–Dielectric Coupling

T. N. Narayanan,[†] B. P. Mandal,[‡] A. K. Tyagi,[‡] A. Kumarasiri,[§] Xaiobo Zhan,[†] Myung Gwan Hahm,[†] M. R. Anantharaman,[⊥] G. Lawes,*[,§] and P. M. Ajayan*[,†]

[†]Department of Mechanical Engineering and Materials Science, Rice University, Houston, Texas 77005, United States

[‡]Solid State Chemistry Section, Chemistry Division, Bhabha Atomic Research Centre, Mumbai 400 085, India

[§]Department of Physics & Astronomy, Wayne State University, Detroit, Michigan 48202, United States

[⊥]Department of Physics, Cochin University of Science and Technology, Kochi 682022, India

S *Supporting Information*

ABSTRACT: The development of methods to economically synthesize single wire structured multiferroic systems with room temperature spin–charge coupling is expected to be important for building next-generation multifunctional devices with ultralow power consumption. We demonstrate the fabrication of a single nanowire multiferroic system, a new geometry, exhibiting room temperature magnetodielectric coupling. A coaxial nanotube/nanowire heterostructure of barium titanate ($BaTiO_3$, BTO) and cobalt (Co) has been synthesized using a template-assisted method. Room temperature ferromagnetism and ferroelectricity were exhibited by this coaxial system, indicating the coexistence of more than one ferroic interaction in this composite system.

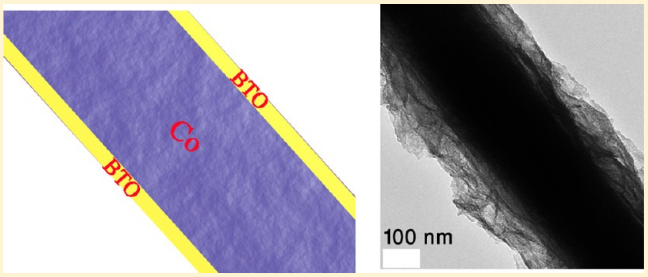

KEYWORDS: *Multiferroic materials, 1D heterostructure, barium titanate nanotubes, Co nanowires, spin–charge coupling, magnetocapacitance*

One-dimensional (1D) nanostructures such as nanotubes and nanowires attract considerable scientific attention because of their novel structure and physical properties, which can differ significantly from their bulk or thin film counter analogues.[1−3] From a practical standpoint, nanowires and nanotubes are the focus of intensive research effort owing to their unique applications in the fabrication of nanoscale devices and interconnects.[4]

Multiferroic materials exhibit more than one ferroic order simultaneously, such as ferromagnetic/antiferromagnetic or ferroelectric/ferroelastic/ferrotoroidic.[5] However, the abundance of intrinsic multiferroic materials is sharply limited by the competing symmetry requirements for each type of ferroic order. Generally, ferroelectricity is associated with an empty outer shell d electrons (known as d^0 ness) while magnetic ordering requires unpaired d or f electrons, i.e., partially filled.[6] While these types of fundamental incompatibilities can make it challenging to identify intrinsic multiferroics, forming nanoscale composites of different ferroic materials to produce multiferroic superstructures provides an alternate method to introduce the desired materials properties. The coupling between the ferroic order parameters can be modulated by heteroepitaxial strain and crystal chemistry.[6,7] The development of magnetoelectric multiferroics, having coexisting magnetic and ferroelectric order, opens the possibility of controlling the magnetic/electric structure using either electric or magnetic fields. This type of cross-control requires a significant coupling between charge and spin or, in other words, a coupling between electric polarization and magnetic moment. This characteristic behavior is of considerable scientific and technological interest, and a number of studies are being conducted to design new multiferroic structures to foster a great understanding of the factors that promote the coupling between magnetic and ferroelectric order parameters.[6−18] Potential applications for multiferroic materials range from multiple-state data storage elements, to magnetically tunable high frequency electrical devices such as filters and oscillators, to electrically tunable microwave magnetic resonance applications, to low frequency, high field magnetic field sensors.[16] The use of multiferroic structures in spintronics is a rapidly developing field of interest, and a number of possible device architectures have been proposed.[17] Epitaxial thin film multilayers are among the most intensively studied artificial multiferroic structures in the literature, since these allow excellent control of the materials properties, but are challenging and expensive to synthesize, since both the order parameters should be stabilized within a few nanometers.

First principle calculations on prototypical heterostructured systems, such as $Fe/BaTiO_3$, have indicated that interfacial

Received: March 1, 2012
Revised: April 18, 2012
Published: April 30, 2012

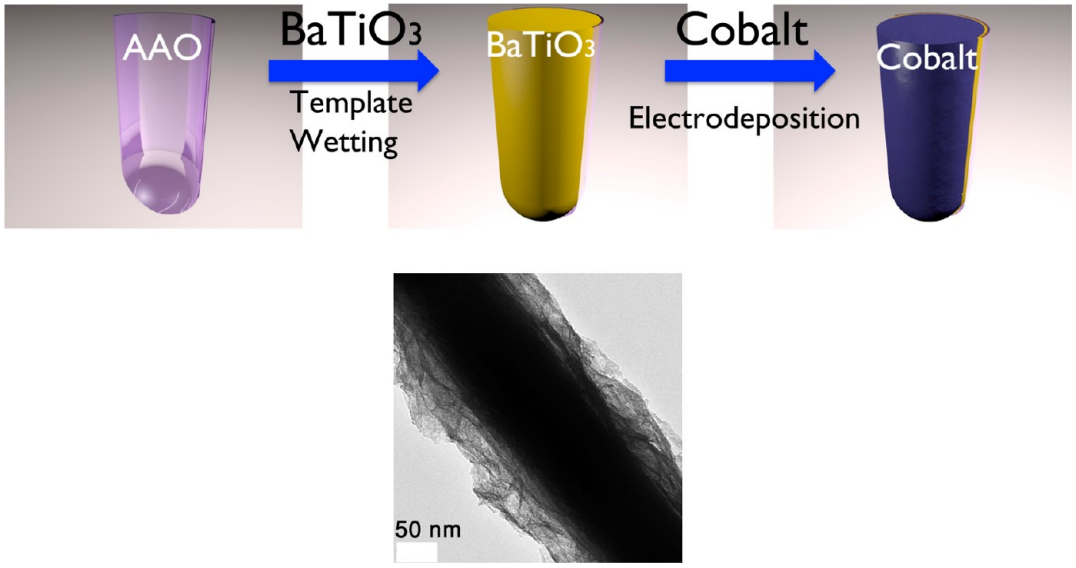

Figure 1. (top) Schematic of the synthesis of Co inside BTO 1D heterostructure. $BaTiO_3$ nanotubes (BTO) have been synthesized using template wetting, and Co NWs have been synthesized by electrodeposition using cobalt sulfate heptahydrate as precursor. (bottom) TEM of Co inside BTO structure after the removal of AAO template.

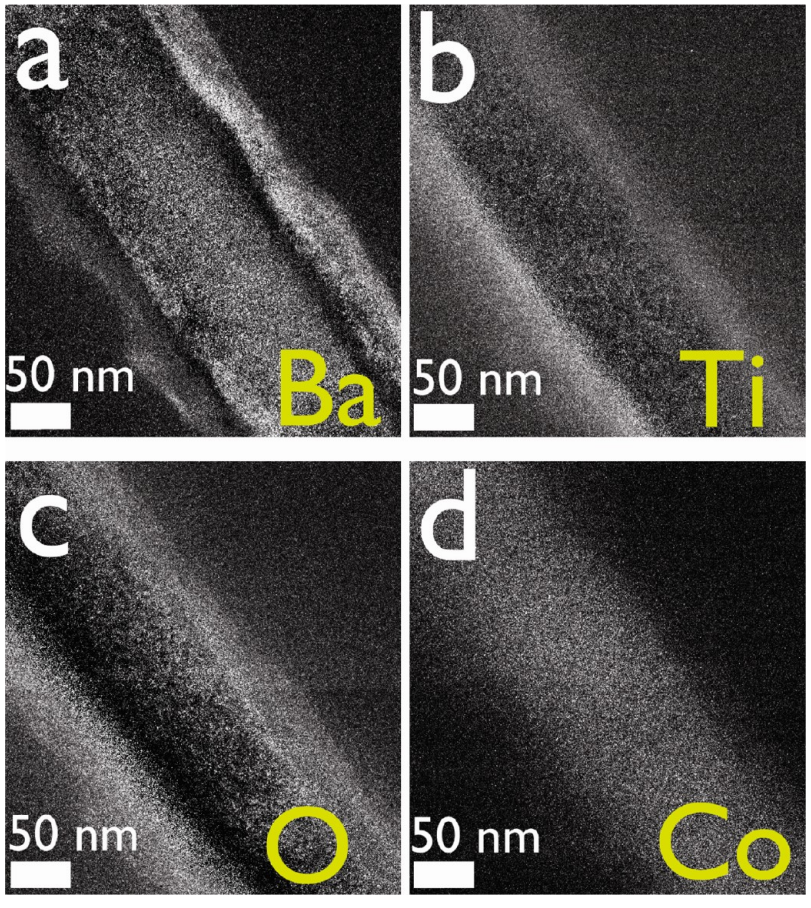

Figure 2. EDS elemental mapping of Co inside BTO heterostructure. The shell contains BTO having a thickness ~80−100 nm, and core contains Co having thickness 150−170 nm.

effects can provide magnetoelectric coupling in these nanoscale structures.[14] Interfacial strain can induce significant charge redistribution at the interface and may cause the ferromagnetic order to become sensitive to the ferroelectric polarization direction. Moreover, it has recently been established that spin-polarized gaps can develop in tunnel barriers that are in contact with ferromagnetic transition metals such as Fe/Co/Ni.[9,11,14]

With this background, we argue that coaxial 1D nanocomposite structures can offer both heteroepitaxy and significant strain effects while at the same time providing

dx.doi.org/10.1021/nl300849u | *Nano Lett.* 2012, 12, 3025−3030

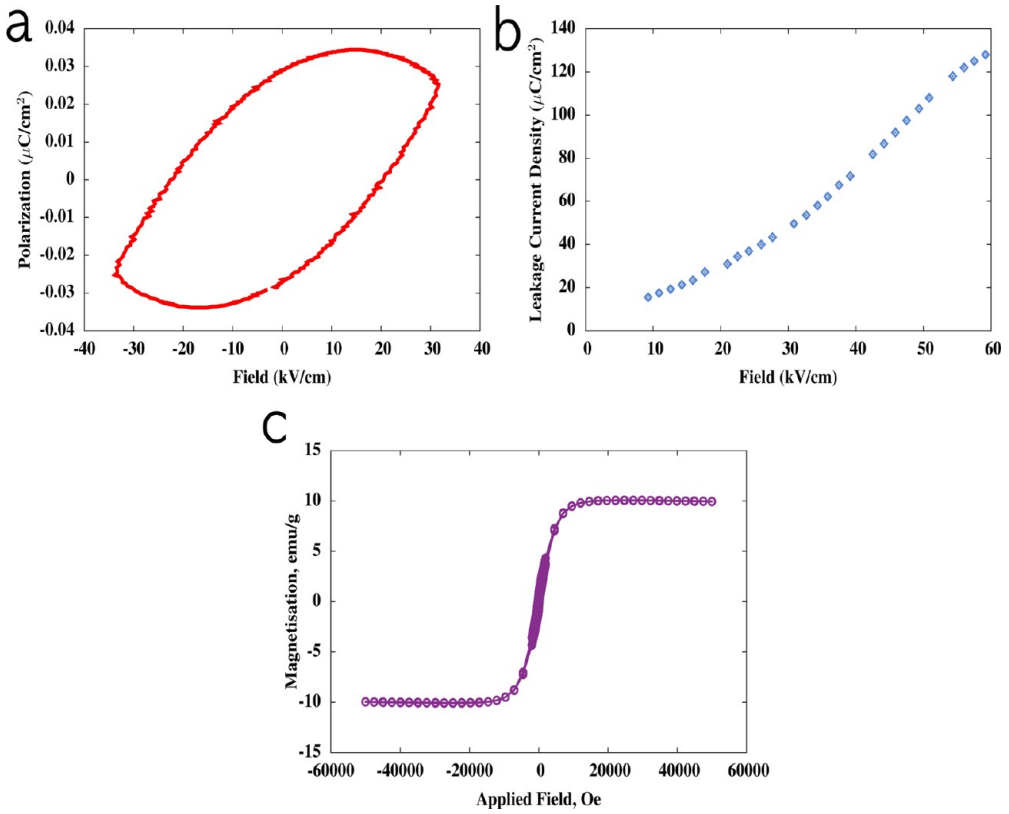

Figure 3. Room temperature (a) ferroelectric $P(E)$ loop of Co inside BTO coaxial structure. The $P(E)$ indicates the inherent ferroelectricity in the sample with a saturation polarization value ~0.036 μC/cm^2. (b) Leakage current measurement carried out on Co inside BTO using ferroelectric loop tracer. (c) $M(H)$ loop of Co inside BTO. The sample shows high coercivity (~350 Oe) compared to bulk Co (~10 Oe), indicating the contribution of uniaxial shape anisotropy of the sample.

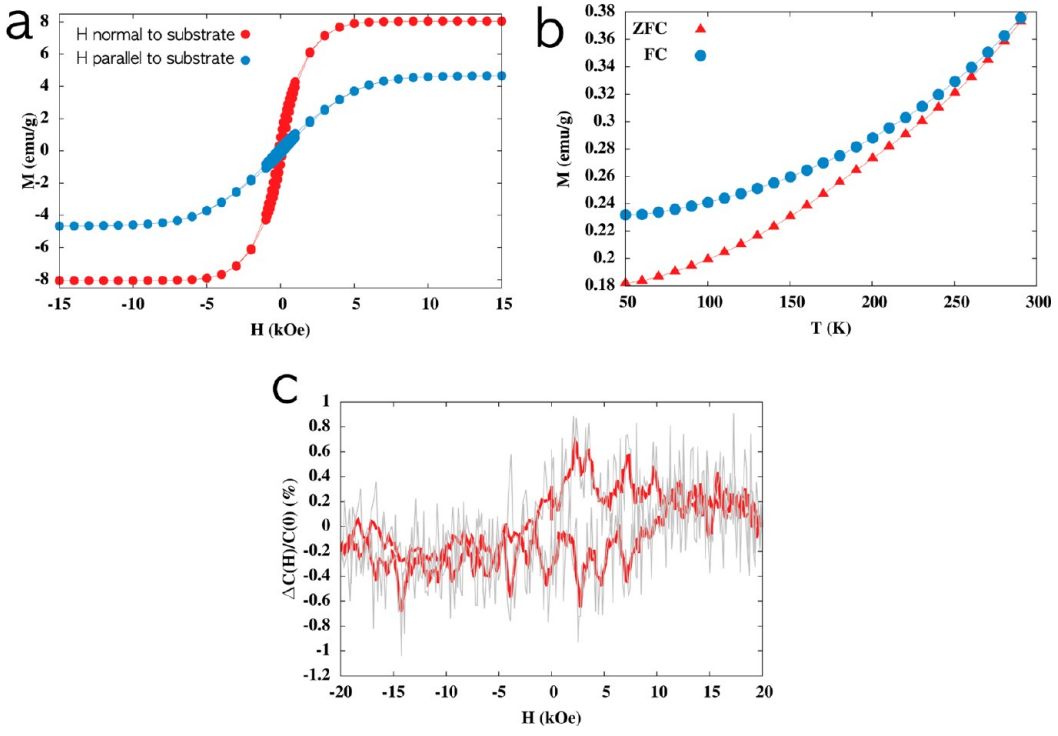

Figure 4. (a) Room temperature $M(H)$ loops of Co inside BTO, both parallel and perpendicular to the substrate (means correspondingly perpendicular and parallel to the nanowires axis), (b) ZFC/FC curves perpendicular to the substrate measured at 100 Oe, and (c) magnetodielectric coupling measurements on Co inside BTO.

dx.doi.org/10.1021/nl300849u | *Nano Lett.* 2012, 12, 3025−3030

more interfacial contact than thin film multilayers. Here we report the synthesis of a nanoscale coaxial multiferroic structure in an alumina (AAO) template by a novel two-step method. Hybrid one-dimensional nanowires containing $BaTiO_3$ nanotubes and Co nanowires (Co NWs)[1] were coaxially grown (hereafter called Co inside BTO) inside AAO pores. We demonstrated the multiferroic nature of this composite, which exhibits a very low leakage current. We also find evidence for higher order magnetoelectric coupling in these nanowires using magnetocapacitance measurements.

Results. A schematic diagram of the formation of Co inside BTO is shown in Figure 1. In this case Co NWs were grown inside BTO by electrodeposition method using cobalt sulfate heptahydrate as precursor. This novel two-step process (explained in the Methods section) can be varied to produce different hybrid structures of BTO and Co. We have also prepared BTO NTs inside Co nanotubes (Co NTs) and other geometries as well, such as an interconnected hybrid structure of Co NT and BTO NT. Co NTs were synthesized by electrodeposition using cobalt acetate as precursor.[19] For the latter hybrid nanostructure, the Co NTs were first grown, and then the template was wetted using BTO sol. Schematic diagrams of the different morphologies of these nanostructures together with the corresponding FE-SEM/TEM images of these structures are shown in the Supporting Information (Figures S5 and S7). TEM image of Co inside BTO is shown in Figure 1 (bottom). SEM images of the Co inside BTO are included in the Supporting Information. The high contrast core in the TEM image (Figure 1) of Co inside BTO represents the ferromagnetic Co NWs, while the outer transparent coating is BTO. The coaxial nature of the structure has been confirmed using EDS elemental mapping (Figure 2). Detailed magnetization $M(H)$ (Figures 3c and 4 and Figure S6) and electric polarization $P(E)$ (Figure 3a,b and Figures S6 and S8) measurements were performed on these hybrid nanostructures, and the room temperature magnetocapacitive response on Co inside BTO was also investigated (Figure 4c).

Discussion. The room temperature ferroelectric ($P-E$) hysteresis loop for this composite is shown in Figure 3a. Determining the ferroelectric properties of materials for such $P-E$ loops can be challenging and can lead to misleading conclusions. It has been previously discussed that materials that show saturation in polarization and have concave region in $P-E$ plot are true ferroelectric.[20] Co inside BTO shows a saturation polarization and concave $P(E)$ curve, thereby indicating the presence of intrinsic ferroelectricity in this sample. This sample also showed a very small leakage current (Figure 3b) compared to other morphologies (Figure S9), an important consideration for device design, so we focused our investigations on this morphology.

The room temperature magnetic hysteresis of the Co inside BTO is shown in Figure 3c. The sample shows a saturation magnetization with a relatively high coercivity ~350 Oe due to the of the 1D geometry of the Co nanowires, leading to considerable shape anisotropy. The bulk coercivity of Co is ~10 Oe,[21] and hence the very high coercivity obtained for Co in BTO can be attributed to the uniaxial shape anisotropy. These measurements confirm that the composites are both ferromagnetic and ferroelectric, so this technique provides a pathway for synthesizing room temperature multiferroic composites. However, we still need to confirm that there is coupling between the magnetic and ferroelectric properties.

Similar magnetic and ferroelectric studies were also conducted on other heterostructures having different morphologies, with the results presented in the Supporting Information. Very briefly, the $M(H)$ loops of all samples always show a high coercivity with significant shape anisotropy. However, the properties of the $P(E)$ curves differ from sample to sample. The structure with BTO inside Co NT showed a very large polarization, but this measurement was likely strongly affected by the high leakage current in this sample due to the metallic (Co) shell. Interestingly, the characteristics of the $P(E)$ curves vary in each different geometry and can be attributed to interfacial effects associated with these structures (Figure 3a and Figures S6 and S8).

To further clarify the effects of sample geometry on the magnetic properties, we measured magnetization curves for fields applied both parallel and perpendicular to the Co inside BTO nanowires and conducted field-cooled (FC)/zero-field-cooled (ZFC) temperature-dependent studies. These data are presented in Figure 4a,b. As shown in Figure 4a, the saturation magnetization is roughly a factor of 2 larger along the Co inside BTO axis as compared to perpendicular to the nanowires. This is consistent with the significant demagnetization field expected for these nanowires and has important implications for incorporating these materials into devices. The largest magnetic response is observed when the field is normal to the templating substrate (parallel to the nanowires), so device geometries incorporating a magnetization parallel to the multilayer stacking direction are likely to be preferred. The ZFC/FC curves show that the magnetization decreases with decreasing temperature, with splitting between these two curves persisting to room temperature. These results are consistent with some superparamagnetic component in the sample, with a blocking temperature well above room temperature. The fact that the ZFC magnetization does not tend toward zero as the temperature is reduced suggests that there is also a significant ferromagnetic component. On the basis of these data, we suggest that the majority of the Co present in the sample acts like a bulk ferromagnetic material, but there is an additional contribution to the magnetic signal from superparamagnetic Co nanoparticles. We do not see any clear evidence for Co nanoparticles in the TEM image shown in Figure 1b, but there could be some small clustering of Co nanoparticles present in the polycrystalline sample during the electrodeposition due to the roughness of BTO template.

Beyond the coexistence of ferromagnetic and ferroelectric order in these multiferroic composites, their suitability for devices requires that these physical properties be coupled. Although we were not able to clearly observe a linear magnetoelectric coupling in these samples, we did find evidence for a higher order magnetoelectric interaction through magnetocapacitive measurements. Figure 4c plots the room temperature capacitance for the nanocomposite sample as a function of magnetic field, with both the electric and magnetic fields applied parallel to the Co inside BTO. We see a small, but significant, hysteresis in the electrical properties of Co inside BTO produced by an applied magnetic field, with a change in the effective dielectric constant of ~1% between increasing and decreasing magnetic field. Although this is a relatively small change in dielectric constant, this type of hysteresis suggests that Co inside BTO devices may be suitable for applications as passive filters, where the zero field permittivity of the system depends on the magnetic history of the sample. Although the magnitude of this effect is not large, the hysteretic behavior may

make the magnetocapacitive coupling in this system amenable to device applications. Furthermore, since these capacitive measurements averaged the signal over a relatively large electrode area, the intrinsic coupling in the nanocomposite may be larger than suggested by these studies.

The contribution from dielectric material alumina (AAO) to a magnetocapacitive signal is also ruled out. Magnetocapacitance measurements on annealed bare AAO templates indicate that AAO has negligible contributions to the magnetocapacitance (Figure S10). Moreover, the capacitance is ∼4 orders of magnitude smaller than that of the Co/BTO sample. AAO also shows a strong diamagnetic response at room temperature (Figure S11).

In conclusion, a new compact 1D nanowire geometry has been proposed for room temperature multiferroic systems. $BaTiO_3$ nanotubes and Co nanowires were coaxially grown inside AAO pores, and their multiferroic nature is demonstrated with a very low leakage current. A high magnetic coercivity of this system along the field parallel to the structure establishes alignment of magnetization along the wire axis, a most important factor for device fabrication. Moreover, a higher order magnetoelectric coupling in this structure is established via magnetocapacitance measurements, indicating the possible tunability of the dielectric permittivity with external magnetic field.

Methods. *Synthesis of BTO/Co Coaxial Structure.* $BaTiO_3$ (BTO) nanotubes are synthesized by a modified template wetting process. Titanium butoxide (Sigma-Aldrich, 97%) is mixed with aqueous solution of barium hydroxide (Sigma-Aldrich, 95%), and the solution is magnetically stirred for 1 h keeping the temperature at 30 °C. The resulting sol is used for template wetting inside AAO template. The resultant wet AAO template is heat-treated at 850 °C for 1 h. The resultant $BaTiO_3$ seems to be phase pure with a perfect perovskoite structure (XRD of $BaTiO_3$ nanotubes after the removal of AAO is shown in Figure S1, XRD studied conducted using Rigaku Kα radiation).

SEM measurements were carried out using FEI quanta 400 high resolution field emission scanning electron microscope, and TEM and EDS measurements were done using JEOL 2100 field emission gun transmission electron microscope.

SEM of the BTO nanotubes is shown in Figure S2. They are short nanotubes with high outer surface roughness due to the roughness of the commercial AAO template.

Co nanowires (Co NWs) can be grown inside AAO template using three-electrode electrodeposition of cobalt sulfate heptahydrate. The electrodeposition was continued up to 2 h in applied potential of −1 V. XRD of Co NWs is shown in Figure S2. The XRD of the nanowires indicates the texturing of Co along (110). Co NWs were electrodeposited inside BTO nanotubes using the above-mentioned method. SEM of the hybrid BTO/Co is shown in Figure S2.

Ferromagnetic Hysteresis M(H) Loop Measurements. The room temperature and low temperature magnetization measurements were carried out using a quantum design magnetic property measurement system (SQUID magnet). The zero-field-cooling and field-cooling measurements were carried out as follows: ZFC measurements were carried out by cooling the sample in zero field up to 50 K, and then the moment is measured while warming in a field of 100 Oe. In FC measurements, the sample is cooled in a field of 100 Oe up to 50 K, and the moment is evaluated while warming up to a temperature ∼300 K. ZFC and FC possess different magnetic ground states.

Ferroelectric Hysteresis P(E) Loop Measurements. The AAO templates were coated with Pt paste, and the ferroelectricity measurement was done on a commercial FE test system (aixACCT: TF-2000). The same instrument is used to measure leakage current. All the ferroelectric hysteresis loops were measured at room temperature at 100 Hz.

Magnetocapacitance Measurements. A thin layer of Ag paint was applied to the top and bottom surface of each film separately to which Au wires were attached to make parallel plate capacitor. An Agilent 4284A LCR meter was used to measure the dielectric signal at a frequency of 30 kHz under a +100 mV excitation, while a Quantum Design PPMS provided the variable magnetic field and temperature control.

■ ASSOCIATED CONTENT

Supporting Information

Figures S1−S11. This material is available free of charge via the Internet at http://pubs.acs.org.

■ AUTHOR INFORMATION

Corresponding Author

*E-mail: ajayan@rice.edu; av4599@wayne.edu.

Notes

The authors declare no competing financial interest.

■ ACKNOWLEDGMENTS

T.N.N. and P.M.A. gratefully acknowledge the financial support from Nanoholdings LLC, Rowayton, CT. Work at Wayne State University was supported by the NSF through DMR-0644823.

■ REFERENCES

(1) Narayanan, T. N.; Shaijumon, M. M.; Lijie, Ci.; Ajayan, P. M.; Anantharaman, M. R. *Nano Res.* **2008**, *1*, 465−473.
(2) Bruce, A.; Scrosati, B.; Jean-Marie, T.; Schalkwijk, W. V. *Nat. Mater.* **2005**, *4*, 366−377.
(3) Benjamin, M.; Song, J. h.; Peidong, Y. *J. Am. Chem. Soc.* **2000**, *122*, 10232−10233.
(4) Gowda, S. R.; Reddy, A. L. M.; Zhan, X.; Ajayan, P. M. *Nano Lett.* **2011**, *11* (8), 3329−3333.
(5) Liu, R.; Zhao, Y.; Huang, R.; Zhao, Y.; Zhou, H. *J. Mater. Chem.* **2010**, *20*, 10665−10670.
(6) Ramesh, R.; Spaldin, N. A. *Nat. Mater.* **2007**, *6*, 21−29.
(7) Valencia, S.; Crassous, A.; Bocher, L.; Gracia, V.; Moya, X.; Cherifi, R. O.; et al. *Nat. Mater.* **2011**, *10*, 753−758.
(8) Catalan, G. *Appl. Phys. Lett.* **2006**, *88*, 102902−3.
(9) Dean, J.; Bryan, M. T.; Schrefl, T.; Allwood, D. A. *J. Appl. Phys.* **2011**, *109*, 023915.
(10) Geprags, S.; Brandlmaier, A.; Opel, M.; Gross, R.; Goennenwein, S. T. B. *Appl. Phys. Lett.* **2010**, *96*, 142509.
(11) Dan, C.; Cai, M.-Q.; Hu, W. Y.; Xu, C. M. *J. Appl. Phys.* **2011**, *109*, 114107.
(12) Sahoo, S.; Polisetty, S.; Duan, C.-G.; Jaswal, S. S.; Tsymbal, E. Y.; Binek, C. *Phys. Rev. B* **2007**, *76*, 092108.
(13) Liu, M.; Li, X.; Imrane, H.; Chen, Y. *Appl. Phys. Lett.* **2007**, *90*, 152501.
(14) Venkataiah, G.; Shirahata, Y.; Itoh, M.; Taniyama, T. *Appl. Phys. Lett.* **2011**, *99*, 102506.
(15) Krishna, S. R. P. S.; Arredondo, M.; Saunders, M.; Ramasse, Q. M.; Valanoor, N.; Munroe, P. *J. Appl. Phys.* **2011**, *109*, 034103−7.
(16) Lawes, G.; Ramirez, A. P.; Varma, C. M.; Subramanian, M. A. *Phys. Rev. Lett.* **2003**, *91* (25), 257208.
(17) Bibes, M.; Barthelemy, A. *Nat. Mater.* **2008**, *7*, 425−426.

(18) Gajek, M.; Bibes, M.; Fusil, S.; Bouzehouane, K.; Fontcuberta, J.; Barthélémy, A.; Fert, A. *Nat. Mater.* **2007**, *6*, 296−302.
(19) Narayanan, T. N.; Shaijumon, M. M.; Ajayan, P. M.; Anantharaman, M. R. *J. Phys Chem. C* **2008**, *112*, 14281−14285.
(20) Scott, J. F. *J. Phys.: Condens. Matter* **2008**, *20*, 021001.
(21) Chikazumi, S. *Physics of Magnetism*; John Wiley & Sons: New York, 1964.